Available online at www.sciencedirect.com
SCIENCE DIRECT
Polymer 47 (2006) 2822–2829
polymer
www.elsevier.com/locate/polymer

An ellipsometric study of polymer film curing: 2,6-Bis(3-aminophenoxy) benzonitrile/4,4′oxidiphthalic anhydride poly(amic acid)

Li Yan [a], Cheol Park [b], Zoubeida Ounaies [c], Eugene A. Irene [a,*]

[a] Department of Chemistry, University of North Carolina, Chapel Hill, NC 27599-3290, USA
[b] NASA Langley Research Center, National Institute of Aerospace, 144 Research Drive, MS-226, 6-West Taylor St, Hampton, VA 23681-2199, USA
[c] Department of Aerospace Engineering, Texas A&M University, 3141 TAMU, College Station, TX 77843-3141, USA

Received 8 December 2005; received in revised form 16 February 2006; accepted 17 February 2006
Available online 10 March 2006

Abstract

The curing of 2,6-bis(3-aminophenoxy)benzonitrile/4,4′oxidiphthalic anhydride ((β-CN) APB/ODPA) has been investigated using spectroscopic ellipsometry on films with various degrees of imidization. Results indicate that much of the film imidization is accomplished at 200 °C and above. Three absorption peaks have been observed (4.1, 5, and 6 eV) which correspond to intra- and inter-molecular optical transitions. A comparison of the film optical constants for the pristine poly(amic acid) and the fully cured polyimide shows film densification upon imidization. A curing timeline has been obtained using in situ real-time spectroscopic ellipsometry, and ellipsometry is shown to serve as a general technique for studying organic film curing.

Keywords: Polymer curing; Spectroscopic ellipsometry; Real-time monitoring

1. Introduction

This research is motivated by the specific desire to use a piezoelectric high-temperature polymer for the development of a flexible, all organic sensor. However, the methods used are generally applicable to polymer film curing studies.

Aromatic polyimides have found wide applications in both aerospace and microelectronics because of the chemical and radiation resistance of the compounds, along with excellent thermal, mechanical, and dielectric properties [1,2]. Based on molecular design and computational chemistry, a series of amorphous piezoelectric polyimides containing pendant, polar functional groups have been developed at NASA Langley for potential use in high-temperature applications [3–5]. One of these, a polyimide containing a single nitrile group, 2,6-bis(3-aminophenoxy)benzonitrile/4,4′oxidiphthalic anhydride (β-CN) APB/ODPA shown in Fig. 1, is the focus of this study. The material is of great interest because it retains more than 50% of its room temperature remnant polarization (P_r, polarization retained after the poling field is removed) at 150 °C for 500 h [6,7].

Polyimide is typically formed by imidization of poly(amic acid) (PAA). (β-CN) APB/ODPA is prepared from 2,6-bis(3-aminophenoxy)benzonitrile ((β-CN) APB) and 4,4′oxidiphthalic anhydride (ODPA) via a poly(amic acid) solution in *N*,*N*-dimethylformamide (DMF), as shown schematically in Fig. 1. Details of the synthesis of (β-CN) APB/ODPA have been described elsewhere [4].

Films of polyimide are often prepared by first forming a film via solution or spin casting solutions of poly(amic acid) precursor onto a substrate and then converting to the polyimide by thermal curing. The properties of polyimide depend strongly on the degree of imidization, which in turn is determined by the curing process. Consequently, in order to produce a reliable polyimide material, it is necessary to develop a curing procedure that is well understood and characterized. For practical reasons, processing temperatures for depositing organic films and fabricating devices are restricted. This motivates current curing studies where a combination of soak time and temperature is sought that would lead to a cured material. The achievement of complete film imidization is crucial because, any remaining, non-imidized PAA in the final product could compromise the device performance and/or jeopardize high temperature stability via continued curing. Moreover, water, which is the by product of curing and any

* Corresponding author. Tel.: +1 919 966 1652; fax: +1 919 962 2388.
E-mail address: gene_irene@unc.edu (E.A. Irene).

0032-3861/$ - see front matter © 2006 Elsevier Ltd. All rights reserved.
doi:10.1016/j.polymer.2006.02.056

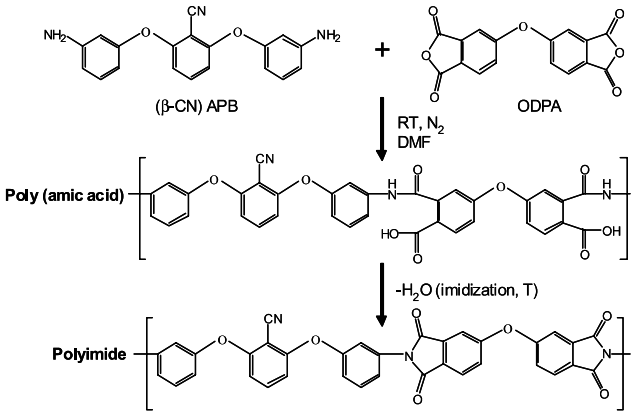

Fig. 1. Schematic of (β-CN) APB/ODPA polymerization.

solvent left behind could potentially reduce the piezoelectric response through relaxation of dipoles, posing risks to device reliability and performance. The extent of cure is dependent upon both temperature and film thickness. Thicker films, for instance, are expected to exhibit more rapid imidization rate due to their higher solvent content and molecular mobility [1]. On the other hand, a slower cure might be expected from more dense films. Due to the wide variability in thin film depositions it would be ideal to monitor the curing in real-time, to ensure complete film imidization in a most energy- and time-efficient manner. Studies at NASA have provided an outline of the curing conditions for (β-CN) APB/ODPA [6,7] and the present research includes in situ real-time diagnostics, in order to provide details about the curing process.

The aims of this study are two-fold: (1) to understand the relationship(s) between the curing process and material properties in particular optical properties and (2) to demonstrate that ellipsometry can monitor the curing process for organic films.

2. Experimental

2.1. Film preparation

In order to obtain the desired film thicknesses, various weight concentrations (2–6%) of (β-CN) APB/ODPA PAA solutions in DMF (anhydrous grade) were used. Films were made by spin coating the PAA precursor at rotation speeds ranging from 2000 to 7000 rpm with the ramping acceleration set to 1950 rpm/s. The substrates included quartz slides (Chemglass), which were cut to 25 mm × 15 mm for UV–Vis absorbance measurements, and single crystal Si wafers. All substrates were cleaned immediately prior to depositions. The Si substrates were cleaned by the RCA method [8] followed by an HF dip, deionized water and blown dry in N_2. The same procedures applied to the quartz slides except that no HF dipping was used. After spinning, the cast films were dried at room temperature overnight to form tack-free films.

2.2. Optical properties determination

Ellipsometry [9,10], a non-destructive, non-invasive optical technique, was used to determine the film optical properties. Reflection ellipsometry measures the change of polarization state of light upon reflection from a sample surface. Ellipsometric measurables, Ψ and Δ, are, respectively, the ratios of the amplitude and phase changes for the p- and s-components of polarized light, and are related to the complex Fresnel reflection coefficients (R) of the sample as follows [9]:

$$\rho \equiv \tan(\Psi)e^{i\Delta} = \frac{R_p}{R_s} \quad (1)$$

where p- and s- correspond to directions parallel and perpendicular to the plane of incidence, respectively. In the general case of a multilayered structure, R_p and R_s arise from the sum of the multiple reflections between each layer [9]. Spectroscopic ellipsometry (SE) measures the complex ratio ρ as a function of photon energy (or wavelength). Because ellipsometry measures ratios, it is highly sensitive to the presence of films thinner than 1 nm. With initial estimates for the unknown layer thickness and/or optical constants, a set of Ψ and Δ values are calculated for the known wavelengths and angles of incidence. The weighted mean square difference between calculated and measured values is calculated, and then minimized using the Levenberg–Marquardt algorithm by varying the model parameters. The thickness and optical constants are then obtained from the regression analysis.

In this work, the optical constants of the polyimide films (with various degree of imidization) were determined using an M-88 multi-wavelength ellipsometry system (J.A. Woollam Co., Lincoln, NE). This system simultaneously acquires a complete spectrum of ellipsometric data at 88 wavelengths covering a 1.62–4.5 eV (276–763 nm) spectrum. The angle of incidence was nominally 70°, and was determined accurately using a thermally oxidized silicon wafer.

2.3. Curing process observations

A vacuum chamber with a custom-made rotating analyzer ellipsometer (RAE) capable of real time ellipsometry, shown in Fig. 2, was used for the curing studies. Films approximately 100 nm thick were exposed to various cure cycles in vacuum (10^{-6} Torr) at a heating rate of 1–1.5 °C/min to produce varying degrees of imidization. Relatively slow ramp rates were employed to minimize bubbles and/or wrinkles formed during the cure.

In order to examine the effects of various curing conditions, samples were heated to different temperatures and/or durations in a step-wise fashion. For each curing process, two PAA samples were placed side-by-side in the chamber: one with PAA on quartz slide (labeled a) and the other with PAA on bare Si (labeled b). The samples on quartz were to be used for UV–Vis absorbance measurements, and the samples on Si were for ellipsometry and FTIR reflectance measurements. Listed in Table 1 is a series of curing recipes conducted on seven pairs of

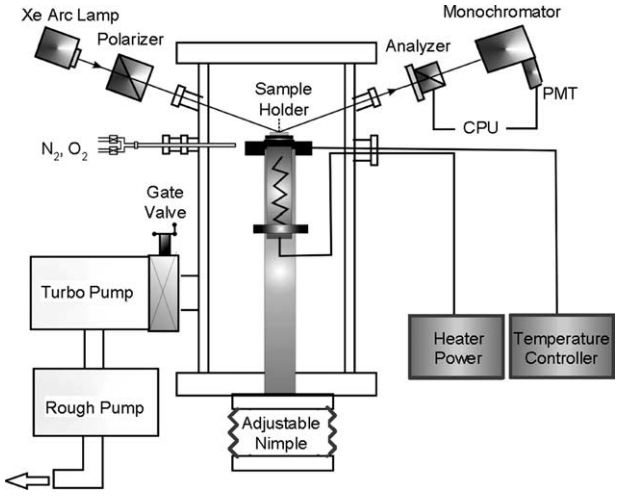

Fig. 2. Schematic of the home-built vacuum system with in situ SE accessories.

identical PAA samples (~100 nm). The final curing step for samples 1 through 5 was at 50, 100, 150, 200, and 240 °C for 1 h, respectively. Samples 6 and 7 underwent the same cure procedure as no. 5 except that they were last cured at 240 °C for 2 and 3 h, respectively. The glass transition temperature (T_g) of this polyimide is around 215–220 °C, depending on the molecular weight and degree of cure [7]. A final maximum cure temperature that is greater than the T_g was necessary to ensure a 100% cure, because the solvent cannot be readily removed below T_g. In addition, previous work by Dezern et al. indicates that optimum mechanical film properties are obtained by limiting the ultimate cure temperature to T_g+20 °C [11], in our case, 240 °C.

2.4. Ex situ film analyses

After each cure cycle samples were removed from the chamber and cooled to room temperature prior to a particular measurement. Apart from ex situ SE, atomic force microscopy (AFM) in tapping mode was used to examine the topographies of the films at various stages of curing over an area of 2 μm× 2 μm using a Nanoscope III Multimode™ AFM (Veeco Instruments Inc., Santa Barbara, CA). The degree of imidization was assessed using results from a Nicolet Nexus 870 FTIR Spectrophotometer (Thermo Electron Co.) in reflection mode. The UV–vis absorption spectra were measured in transmission using a computer controlled Shimadzu UV-1601 spectrophotometer. In addition, X-ray data were taken on the pristine and the 100% cured PAA films to study the effect of curing on the ordering of the film structure.

Table 1
Curing conditions for seven pairs of PAA samples (~100 nm)

Samples	50 °C (1 h)	100 °C (1 h)	150 °C (1 h)	200 °C (1 h)	240 °C (h)
1a, 1b	√				
2a, 2b	√	√			
3a, 3b	√	√	√		
4a, 4b	√	√	√	√	
5a, 5b	√	√	√	√	1 h
6a, 6b	√	√	√	√	2 h
7a, 7b	√	√	√	√	3 h

2.5. In situ SE monitoring

In situ spectroscopic ellipsometry was performed as a function of curing time during a single complete curing process. As opposed to previous ex situ SE measurements on samples with various degrees of imidization, real-time monitoring offers a more detailed examination of the process, with the benefit of not exposing samples to the ambient prior the measurement. The same curing recipe as for sample 6b (Table 1) was repeated on a separate PAA film (~100 nm), and SE data were taken at various times over a spectral range of 1.6–4.6 eV (270–775 nm), using the pre-configured home-built RAE system shown in Fig. 2. A 70° angle of incidence was set on the goniometer base.

3. Film curing results and discussion

3.1. Ex situ studies

3.1.1. FTIR spectroscopy

The FTIR spectral changes observed upon curing the PAA at elevated temperatures provide evidence for the ring closure reaction and thus the formation of polyimide. By simultaneously monitoring the bands associated with amide (–NH–CO–) in the PAA and the imide (N–CO–) modes in the polyimide, the degree of imidization can be assessed as a function of curing conditions.

Fig. 3 shows the effect of curing temperature on the FTIR spectra of the (β-CN) APB/ODPA films. Data on pristine PAA

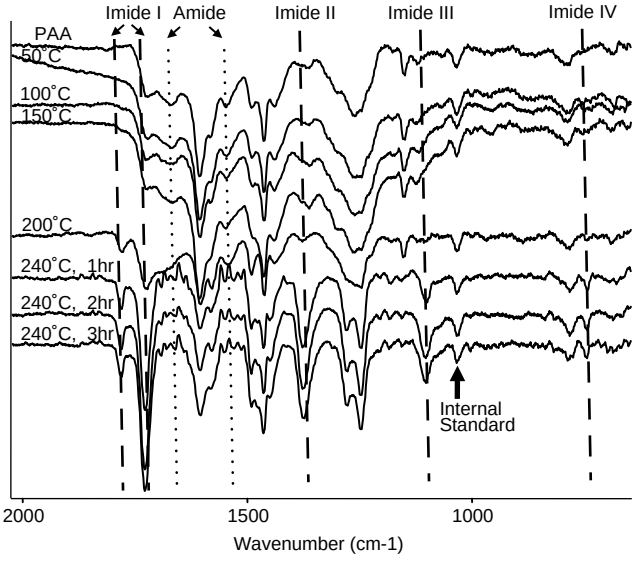

Fig. 3. FTIR spectra of pristine and cured PAA with various degrees of imidization (1b through 7b in Table 1).

is also included for comparison (topmost spectrum). A number of structure independent vibrational bands have been identified in the literature: imide I, II, III, and IV, all of which are linked to the invariant imide portion of aromatic imide compounds [12,13]. Imide I is composed of two bands, 1770–1780 and 1720–1730 cm^{-1}, which correspond to the carbonyl (C=O) absorption. The doublet nature stems from the coupling of the in-phase (higher frequency) and out-of-phase (lower frequency) vibrations of the two carbonyl groups. Imide II, III, and IV modes correspond to axial, transverse and out-of-phase displacements of the nitrogen with respect to C=O, respectively. The IR spectra of the (β-CN) APB/ODPA polyimide (Fig. 3) have imide vibrations at 1780/1724 cm^{-1} (imide I), 1375 cm^{-1} (imide II), 1100 cm^{-1} (imide III) and 740 cm^{-1} (imide IV).

The imidization process was characterized by monitoring the changes in the imide peaks at 1780, 1724, and 1375 cm^{-1}. The band at 1032 cm^{-1}, which represents the vibration of the aromatic moieties, was considered to be an internal standard, since it remains unchanged during curing [14]. As can be seen, the 1780 cm^{-1} C=O symmetrical stretching vibration mode is barely observed below 200 °C. This means that the film imidized very little below this temperature. At 200 °C and above, this peak emerged; its intensity increased with increasing curing temperature and eventually leveled off at 240 °C. In the meanwhile, the intensities of the amino bands at 1660 (amide I) and 1550 cm^{-1}(amide II) [14] were found to decrease with increasing curing temperature. At 240 °C, these two amide modes of vibration disappeared entirely. Apparently, below 240 °C, the film has only partially imidized. The three primary imide peaks at 1780, 1724, and 1375 cm^{-1} remain unchanged after curing at 240 °C for 2 h, indicating that imidization was already completed in sample 6 (Table 1). Prolonged heating at this temperature (sample 7) did not seem to affect the IR spectra in any detectable way; a 100% PAA-to-PI conversion was thus accomplished for both samples 6 and 7. The difference between the IR spectra for samples 5 and 6 (or 7), though subtle, does exist, with the latter having a slightly more intense 1724 cm^{-1} imide I peak.

3.1.2. UV–Vis spectroscopy

The measured UV–Vis absorbance spectra of cured samples 1a through 7a are shown in Fig. 4. For clarity, separate lines represent data from four (1a, 4a, 5a, and 7a) out of the seven cured plus pristine PAA samples. As can be seen, the spectra consist of three broad peaks centered at about 4.1 eV (302 nm), 5 eV (248 nm) and 6 eV (207 nm) with a tail extending into the visible. The causative optical transitions may take place within one single molecule (intramolecular transitions) or between different molecular chains (intermolecular transitions). The thermal cure has two major effects on the molecular structure of polyimide. One is to promote the formation of imide rings (i.e. imidization), and the other is to cause a change of the molecular ordering and free volume between different molecular chains [15]. Both of these effects can appear in the UV–Vis absorbance spectra. The formation of imide rings introduces new electronic states, thus giving rise to new

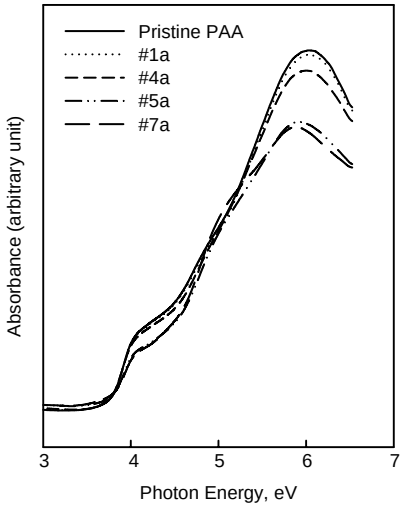

Fig. 4. UV–Vis absorbance spectra of pristine and cured PAA with various degrees of imidization (1a, 4a, 5a, and 7a in Table 1). Note: (1) eV = 1240/λ (nm); (2) the scale for absorption is linear.

absorption peaks in the spectra [15]; whereas, the physical rearrangement of molecular chains, either within themselves or relative to the others, will not. Changes in the degree of intermolecular ordering affect the intermolecular charge transfer between chains and consequently the appearance of the UV–Vis absorbance spectrum.

The UV–Vis absorption spectra for a series of polyimide compound materials have been previously measured by LaFemina et al., and the spectroscopically parameterized CNDO/S3 model used to provide a detailed quantitative description of the spectra [16,17]. As seen in Fig. 4, the ~6 eV (207 nm) absorption peak in the fully cured PI (sample 7a) appears in the other uncured samples (sample 1a–5a) as well, but at higher energies. This peak in the fully cured polyimide could to be due to π–π* intramolecular transitions [16]. It consists of a strong π–π* transition as its major component and is surrounded by other weaker π–π* transitions, close in energy, contributing to the broad nature of the peaks. Sample 7a basically consists of polyimide only, whereas samples with lower degrees of imidization (1 through 5) are essentially a mixture of polyimide and its precursor PAA. There have been reports based on X-ray photoelectron (XPS) spectra which show that the π-states in polyimides are different from those in PAA [18]. The shift of the peak position in Fig. 4 indicates the changes of such π-states during cure. The low-energy peak at ~4.1 eV (302 nm) arises primarily from the π–π* transition from the highest-occupied molecular orbital (HOMO) to the lowest-unoccupied molecular orbital (LUMO) [16]. It undergoes a red shift that is similar to that of the intramolecular transition peak at ~6 eV (207 nm), though much smaller in magnitude.

On the other hand, the ~5 eV (248 nm) absorption peak in Fig. 4 exhibits fairly different behavior with increasing curing temperatures. It starts out as an absorption shoulder for the pristine PAA and gradually emerges as a clearly discernible peak though still broad in sample 7a. Samples 5a and 7a have similar degrees of imidization (based on the FTIR data above);

their chemical structures are thus largely the same. Therefore, we conclude that the changes of this 5 eV (248 nm) absorption peak are due to changes of interactions between different molecular chains. The formation of intermolecular charge–transfer complexes in polyimide has long been recognized [19,20]. The 5 eV (248 nm) absorption peak in sample 7a is more intense because the intermolecular transitions between neighboring molecular chains are stronger with the fully cured polyimide. Several investigators have reported that the ordering of polyimide films changes as a result of curing [21–24]. The X-ray diffraction patterns on our cured films have shown some degrees of intermolecular ordering enhancement via the diffraction peak at $2\theta = 15°$, which explains the increasingly stronger intermolecular charger transfers and thus the changes to this 5 eV absorption peak.

3.1.3. Ex situ SE

Fig. 5 displays ex situ ellipsometric raw data (Ψ and Δ) taken from the cured PAA samples 1b through 7b (Table 1). Data on the pristine PAA sample are also included for comparison (leftmost curves). The blue shifts, indicated by the arrows, are observed for both spectra. Below 200 °C (sample 4b), the shifts were small and indicated little film imidization. At 200 °C and above, the films underwent significant changes, but eventually stabilized after curing at 240 °C for 2 h (sample 6b). As illustrated in Fig. 5, additional curing at this temperature had no discernible effects on the films; the SE data for samples 6b and 7b (3 h at 240 °C) overlap each other. This agrees well with previous FTIR and UV–Vis absorbance results.

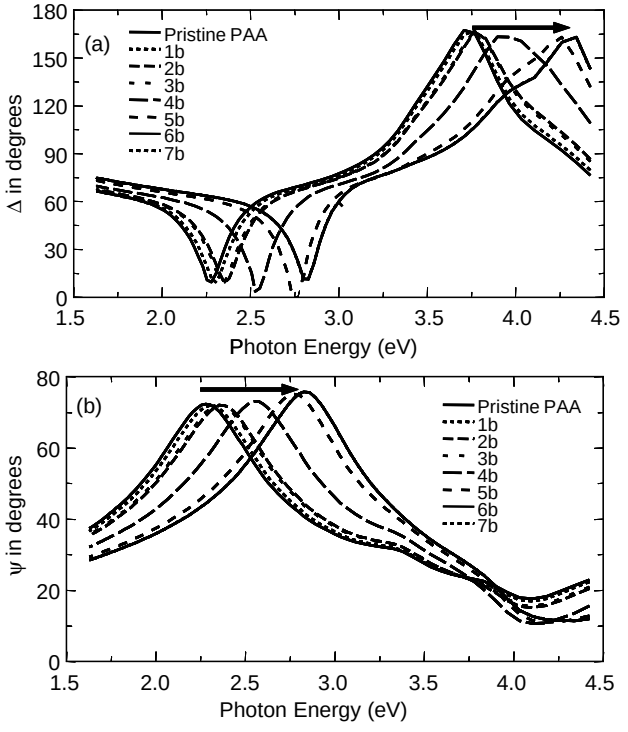

Fig. 5. Ex situ SE raw data of the pristine and cured PAA film with various degrees of imidization (1b through 7b in Table 1). (a) Ψ (b) Δ. Note: eV = 1240/λ (nm).

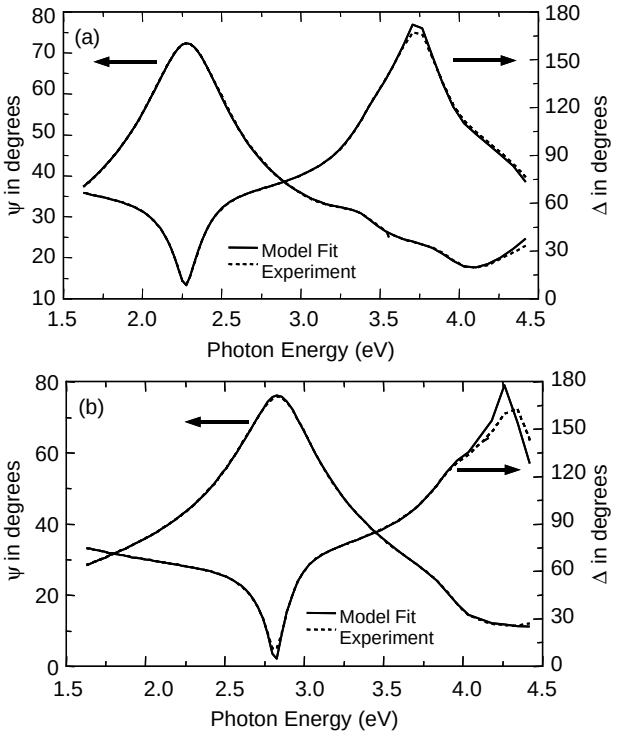

Fig. 6. Regression model fits to experimental data for (a) the pristine PAA and (b) fully cured PI films. Note: eV = 1240/λ (nm).

3.1.4. Optical properties determination

Fig. 6(a) and (b) shows respectively, SE data, combined with regression analysis model fits, for the pristine PAA (leftmost curves in Fig. 5) and fully cured polyimide films (samples 6 and 7; last curves in Fig. 5). A Cauchy formula was first employed over the spectral range for photon energies less than ~3.5 eV (355 nm) where the film is transparent. With the film thickness determined from the visible region, a starting point for the film dielectric function ε was obtained by conducting a 'point-by-point' fit at each measured wavelength assuming no surface overlayers. The dispersion of ε was approximated by a summation of four Gaussian oscillators. The dielectric constant ε has the following form:

$$\varepsilon = N^2 = \varepsilon_1 + \mathrm{i}\varepsilon_2, \tag{2}$$

where N is the complex refractive index ($N = n + \mathrm{i}k$ where n is the real refractive index and k is the absorption constant) and the real and imaginary parts of the dielectric function are given as:

$$\varepsilon_1 = \frac{2}{\pi} P \int_{R_g}^{\infty} \frac{\xi \varepsilon_2(\xi)}{\xi^2 - E^2} \mathrm{d}\xi \tag{3}$$

and

$$\varepsilon_2 = A\mathrm{e}^{-(E-E_c/\mathrm{Br})^2} - A\mathrm{e}^{-(E+E_c/\mathrm{Br})^2}$$

where P denotes the principle value of the integral, A is oscillator amplitude, E_c is center energy, and Br is a broadening

Table 2
Gaussian oscillator coefficients for (a) pristine PAA and (b) fully cured PI valid 1.62–4.5 eV (276–763 nm)

	A (Amplitude)	E_c (eV)	Br (eV)
(a) Pristine PAA			
1	0.032708	3.1251	0.77625
2	0.35003	4.047	0.28569
3	0.25827	4.265	0.26184
4	1.8363	5.1	1.0672
(b) Fully cured PI			
1	0.0079996	3.1032	0.61262
2	0.040035	3.6905	0.26948
3	0.19411	4.047	0.26178
4	2.2888	5.1	1.368

term. Note that the real part ε_1 is computed using the Kramers–Kronig (KK) relation.

A commercial modeling program [25] was used to add dielectric function terms systematically while maintaining KK consistency. Dispersion in the real part of the dielectric function was included by addition of a zero-broadening Lorentzian oscillator 'pole' at 11 eV. According to the Kramers–Kronig relation, no absorption is isolated; i.e. absorption in one spectral range is always associated with dispersion over a broader range. The pole accounts for this dispersion in the visible range due to UV absorption that is outside the spectral range of the instrument. Listed in Table 2 are the best-fit Gaussian oscillator coefficients for the (β-CN) APB/ODPA films in Fig. 6. As seen, excellent fits were achieved for both pristine PAA (Fig. 6(a)) and fully cured PI films (Fig. 6(b)), with a mean square error (MSE) of only 4.9 and 2.7, respectively. The slight mismatches at the higher energy end of the spectra (especially in Fig. 6(b)) are due to the difficulty in fitting the strong absorptions around the edges of the instrument's spectral capability. Note that all the SE data analyses conducted in this work assumed homogeneity through film thickness.

The pristine PAA film thickness was subsequently determined by SE to be 99.7 nm with a 3.5% non-uniformity over the measured area. The small thickness variation was also evidenced from the AFM image (2 μm×2 μm) in Fig. 7(a), which indicates a smooth film surface with about 0.22 nm root mean square (rms) roughness. Much like their PAA predecessor, the 100% cured polyimide films (samples 6b and 7b) are smooth as well, shown by AFM in Fig. 7(b). The rms roughness increased just slightly, from previous 0.22 nm for the pristine PAA to 0.37 nm for the fully cured PI film. On a larger scale of 20 μm×20 μm, AFM yielded a similar rms roughness change (from 0.32 to 0.38 nm). This indicates that films of PAA and fully cured PI have comparable roughness and thickness uniformity; i.e. curing does not significantly roughen the surface for the conditions used in this work.

Fig. 8 shows the final determined optical constants (in terms of n and k) for the pristine PAA and 100% cured polyimide films. As a result of curing, the film indices of refraction increased appreciably over the measured spectral range (Fig. 8(a)). Generally, the refractive index of a polymer depends on its molecular refraction and molecular volume; i.e.

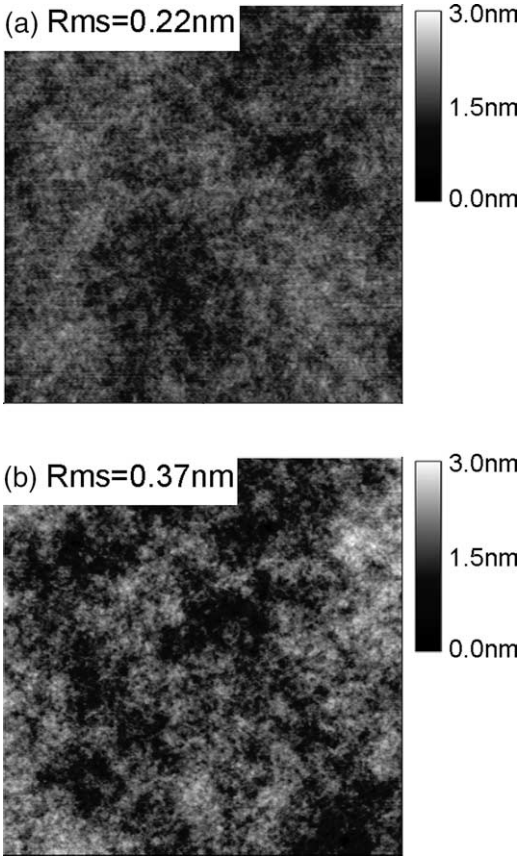

Fig. 7. AFM images (2 μm×2 μm) of ~100 nm (a) PAA and (b) fully cured PI films.

polarizability of the atoms present in a unit volume of the polymer backbone [26]. A decrease in the free volume increases the number of polarizable groups in a unit volume and hence the refractive index [27]. An estimate of the film densities, ρ, from the Lorentz–Lorenz relationship ($\rho = K(n^2-1)/(n^2+2)$, where K is a constant) [28] indicates a film densification by approximately 3.3%. This density increase compared with the ~24% thickness decrease (from 99.7 to 75.5 nm) indicates that much of the thickness decreases is due to loss of solvent and a small portion to actual densification of the material.

3.2. In situ SE monitoring

In situ SE was conducted in order to provide a timeline for the curing process that is missing from the ex situ measurements presented above, to provide results on a single sample not exposed to the atmosphere once the curing was started, and to provide a means for non-destructive process monitoring.

Fig. 9 shows the time evolution of ellipsometric Ψ and Δ data taken at 3.65 eV (340 nm) on a separate ~100 nm PAA sample under cure. Data at other wavelengths over the measured spectral region of 1.6–4.6 eV (270–775 nm) exhibited similar characteristics and will not be presented here. As opposed to ex situ data, a complete curing process was

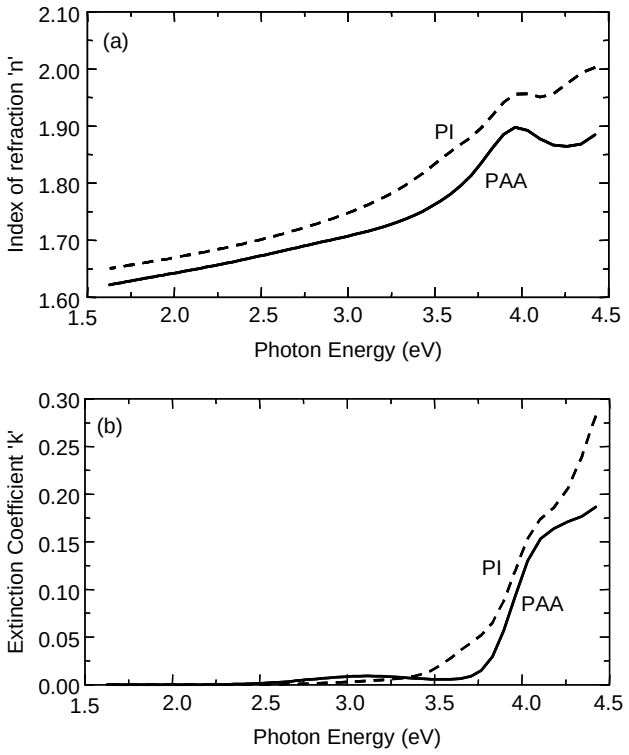

Fig. 8. Optical constants of ~100 nm PAA and 100% cured PI films. (a) n (b) k. Note: eV = 1240/λ (nm).

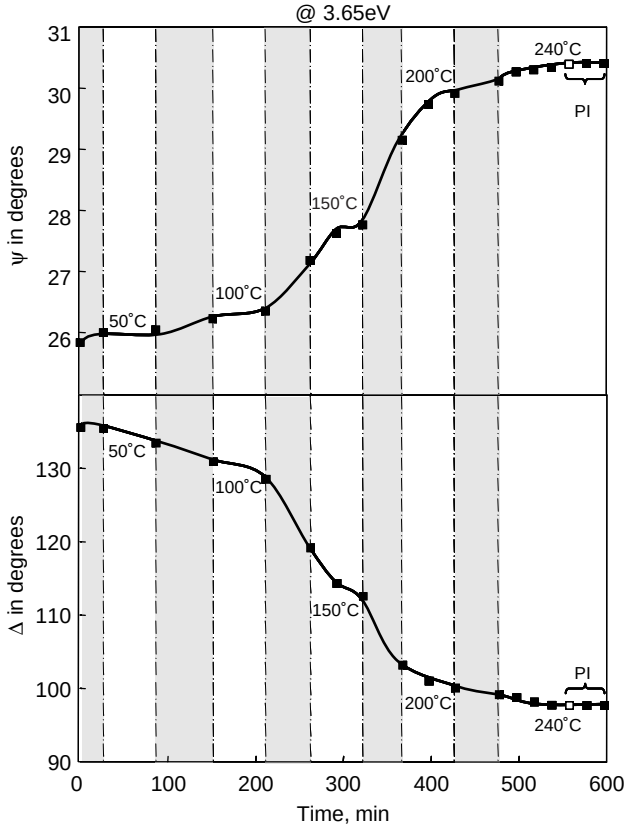

Fig. 9. In situ SE monitoring of a complete (β-CN) APB/ODPA curing process. (a) Ψ and (b) Δ versus time at 3.65 eV (340 nm).

Table 3
The actual time spent at and to each T domain in Fig. 9

Temperature (T), °C	Time to T, min	Time at T, min
50	26	60
100	65	60
150	51	60
200	45	60
240	50	120

recorded with in situ SE, covering both at-temperature time and temperature transient time (grey areas in Fig. 9) to achieve the set-point temperature. Table 3 lists the actual time spent at and to each T domain for the curing process under study. Adding all times yields a total cure time of 597 min (~10 h). Note that in situ SE data were taken in real time at the cure temperatures, rather than at room temperature as for previous ex situ measurements. A question thus arises as to the temperature dependence of film optical properties. A photon energy of 3.65 eV was chosen for in situ ellipsometric data illustration because the dielectric function for the Si substrate is T insensitive at this photon energy [29]. As such, the evolution of Ψ and Δ in Fig. 9 was attributed predominantly to the development of (β-CN) APB/ODPA film from the PAA film. Meanwhile, with reference to the room-T ex situ SE data in Fig. 5, ellipsometric data (Δ in particular) are sensitive to curing at this photon energy. Thus a real-time ellipsometric measurement at 3.65 eV yielded an accurate monitoring of a complete curing process, where T increased consecutively up to 240 °C.

The squares (filled and open) in Fig. 9 represent the actual ellipsometric data points collected subsequently at room temperature (t = 0, corresponding to the pristine PAA), 50, 100, 150, 200, and 240 °C. According to previous ex situ data analyses, not much happened to the film below 200 °C; SE measurements were thus conducted at progressively smaller time intervals as the curing proceeded. At the final 240 °C temperature, a total of 7 data sets in 20 min intervals were collected. As seen, Ψ increased while Δ decreased in a nearly step-wise fashion as a result of curing. This agrees with the blue shifts observed from previous ex situ SE data (Fig. 5). The transient time regimes (grey areas) are marked by distinctly sharper gradients than those observed in the at-temperature domains following immediately behind. After 80 min of curing at 240 °C, corresponding to the third to last data points in Fig. 9 (open squares), both Ψ and Δ curves started leveling off and no changes were detected afterwards, an indication of complete film imidization. This is compared with the 120 min curing period from ex situ curing data for a similar process. This discrepancy is due to the lack of ex situ data for the 1–2 h time interval at 240 °C.

It is instructive to compare the optical properties measured at cure temperature (from in situ SE) versus those at room temperature (from previous ex situ SE) for the fully cured polyimide films. For highly accurate results the temperature dependence of the dielectric constant for Si is required. For the present purpose of illustrating the curing process we assumed the same room-T optical constants and varied only the film

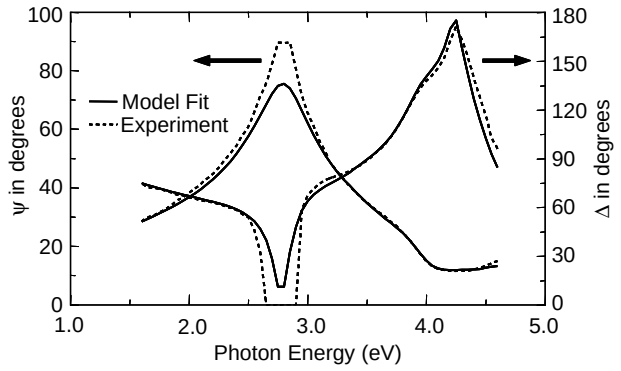

Fig. 10. Regression fits of the SE data taken in situ on the fully cured polyimide film, assuming the room-T film optical constants (Fig. 8). Note: eV = 1240/λ (nm).

thickness in the regression analysis of the SE data taken in situ on the fully cured polyimide film. This led to an acceptable fit, shown in Fig. 10. The final as-determined film thickness was 77 nm, which agrees well with the 76 nm value determined ex situ. The ~1 nm thickness increase was likely due to thermal expansion at higher temperatures. As seen in Fig. 10, the problematic fit areas lie near the peaks and valleys where the response is most sensitive.

Notwithstanding the inherent inaccuracies with in situ real-time SE observations the time evolution of the curing process can be obtained. With in situ SE, an accurate timeline was obtained for the curing of (β-CN) APB/ODPA films and the end point obtained which is a decided advantage of real-time process monitoring. It is clear that in situ SE results alone are usually insufficient, but when combined with more accurate ex situ experiments, the combination provides a complete picture of the curing process.

4. Conclusions

(β-CN) APB/ODPA films with various degrees of imidization were studied ex situ by FTIR, UV–Vis absorbance spectroscopy, ellipsometry, and AFM, yielding an overall picture of the film development at cure time, chemically and physically. Results showed that much of the curing was accomplished at and above 200 °C, when the films became less rigid. Three absorption peaks, located at 4.1, 5, and 6 eV, were identified in the UV–Vis spectra for both poly(amic acid) and fully cured polyimide films. The peaks at 4.1 and 6 eV are due to intramolecular optical transition, whereas the 5 eV peak represents an intermolecular transition.

Gaussian oscillators were used successfully to fit for the film optical constants for both pristine PAA and fully cured PI. The film indices of refraction increased upon imidization, whereas the thickness decreased by about 24%, which is an indication of film densification or free volume decrease. Despite this large change the curing process did not substantially affect the film surface quality. This is important, because roughness could potentially be detrimental to device operations; a mild process is thus always desirable to ensure as smooth of a surface as possible.

In situ SE provided an accurate timeline for the film curing and the present study provides a means to achieve the cured endpoint. For the ~100 nm PAA film investigated in this work, 80 min of baking time at the final 240 °C temperature was necessary to ensure a complete film imidization.

Acknowledgements

This work was supported in part by the NASA University Research, Engineering and Technology Institute on Bio Inspired Materials (BIMat) under award No. NCC-1-02037.

References

[1] Wilson D, Stenzenberger HD, Hergenrother PM, editors. Polyimides. New York: Chapman and Hall; 1990.
[2] Feger C, Khojasteh MM, Htoo MS, editors. Advances in polyimide: science and technology. Boca Raton, FL: CRC Press; 1993.
[3] Simpson JO, Welch SS, Clair TL. Proc Mater Res Soc Symp: Mater Smart Syst II 1995;413:351–6.
[4] Simpson JO, Ounaies Z, Fay C. Proc Mater Res Soc Symp: Mater Smart Syst II 1997;459:59–64.
[5] Ounaies Z, Park C, Harrison JS, Smith Jr JG, Hinkley J. SPIE Proc Smart Struct Mater 1999;3669:171–8.
[6] Park C, Ounaies Z, Su J, Smith Jr JG, Harrison JS. Proc Mater Res Soc Symp: Mater Smart Syst II 1999;600:153–8.
[7] Park C, Ounaies Z, Wise KE, Harrison JS. Polymer 2004;45:5417–25.
[8] Kern W, Puotinen D. RCA Rev 1970;31:187–206.
[9] Azzam RMA, Bashara NM. Ellipsometry and polarized light. New York: North-Holland; 1977.
[10] Humlíček J. Polarized light and ellipsometry. In: Tompkins HG, Irene EA, editors. Handbook of ellipsometry. New York: William Andrew Publishing; 2005. p. 77.
[11] Dezern JF, Croall CI. NASA technical memorandum; 1991. p. 104178.
[12] Dine-Hart RA, Wright WW. J Appl Polym Sci 1967;11:609–27.
[13] Dine-Hart RA, Wright WW. Makromol Chem 1971;143:189–206.
[14] Pramoda KP, Liu S, Chung TS. Macromol Mater Eng 2002;287:931–7.
[15] Kan L, Kao KC. J Chem Phys 1993;98:3445–51.
[16] LaFemina JP, Arjavalingam G, Hougham G. J Chem Phys 1989;90:5154–60.
[17] LaFemina JP, Kafafi SA. J Phys Chem 1993;97:1455–8.
[18] Kowalczyk SP, Stafström S, Brédas JL, Salaneck WR, Jordan-Sweet JL. Phys Rev B 1990;41:1645–56.
[19] Gordina TA, Kotov BV, Kolninov OV, Pravednikov AN. Vysokomol Soyed B 1973;15:378–83.
[20] Kotov BV. Zh Fiz Khim 1988;62:2709–27.
[21] Endo A, Yada TJ. Electrochem Soc 1985;132:155–8.
[22] Takahashi N, Yoon DY, Parrish W. Macromolecules 1984;17:2583–8.
[23] Feger C. Society of Plastic Engineers ANTEC Technical Papers; 1987. p. 967–87.
[24] Jou JH, Huang PT. Macromolecules 1991;24:3796–803.
[25] WVASE32® Software manual, J.A. Woollam Co., Inc. (unpublished).
[26] Ku CC, Liepins R. Electrical properties of polymers. Munich: Hanser Publishers; 1987.
[27] Hougham G, Tesoro G, Viehbeck A. Macromolecules 1996;29:3453–6.
[28] Pliskin WA. J Vac Sci Technol 1977;14:1064–81.
[29] Irene EA. In situ real-time characterization of surface and film growth processes via ellipsometry. In: Auciello O, Krauss AR, editors. In situ real-time characterization of thin films. New York: Wiley-Interscience; 2001. p. 77.